Unknotting of a Polymer Strand in a Melt

Eung-Gun Kim*,† and Michael L. Klein

Center for Molecular Modeling and Department of Chemistry, University of Pennsylvania, Philadelphia, Pennsylvania 19104-6323

Received July 29, 2003
Revised Manuscript Received January 21, 2004

Introduction. In the world of macromolecules there are two basic topological constraints: intramolecular knots, which have been well-studied[1−4] particularly in the case of DNA, and intermolecular entanglements, which are prevalent in synthetic polymers, affecting almost every aspect of their behavior.[5] Experimentally, it is difficult to separate topological from biological components in the dense intracellular state where DNA knots should undergo large conformational changes during various reactions with other macromolecules.[6] A similar situation obtains concerning the influence of knots in entanglement-dominated polymer melts. It is therefore timely to employ computer simulation to explore the interplay of knots and entanglements in a dense macromolecular system. To this end, we have carried out simulation studies on polyethylene (PE) melts containing knots, which serve as an ideal model system exhibiting both intra- and intermolecular topological constraints.

In sufficiently long polymer chains open knots exist in loose form.[7] However, tight knots may be produced from loose knots during quenched crystallization from the melt or under strong longitudinal shear flows in solution.[8] In contrast to circular knots, in which the knotted region is highly localized in the relaxed state,[9−11] tight open knots are only transient, as modeled recently for the case of a short isolated chain by experiment.[12] Such knots are driven entropically[13] to expand and untie. Thus, the untying of a tight knot, confined in a melt or concentrated solution, is expected to necessarily involve the relaxation of intermolecular entanglements. The unknotting of a polymer strand also provides a molecular perspective on the *security* of a knot, a key property which, along with its *strength*, characterizes a macroscopic knot.[14,15] The latter has been much studied recently at a molecular level.[16,17]

Computation. We used a united-atom force field[18] to model the individual PE chains. Monodisperse PE melts were prepared under three-dimensional periodic boundary conditions. Initial guesses for the MD runs were prepared and fully equilibrated on a second-nearest neighbor diamond (2nnd) lattice using a Monte Carlo (MC) algorithm[19] designed to reproduce conformational properties of rotational isomeric state (RIS) chains[20] and bulk densities. Knotted chains were formed by growing from both exit points of a trefoil knot structure with the smallest size, which was generated separately on the diamond lattice. The knot portion of a knotted chain was excluded from MC moves. During subsequent NPT and NVT MD equilibration runs in continuum space, the knotted portion was geometrically constrained with harmonic springs (distance constraints on six pairs of backbone atoms) such that the trefoil knot retains its size at 43 backbone atoms but can release strains. Following equilibration, multi-nanosecond MD trajectories were generated. The systems studied were M (N) = 53 (25), 57 (25), 65 (22), 85 (14), 105 (13), 141 (11), 209 (7), and 293 (8), N being the number of chains in each system with length M carbon atoms. Six to seven independent samples were prepared for each chain length. All simulations including production runs at NVT were carried out at 448 K.

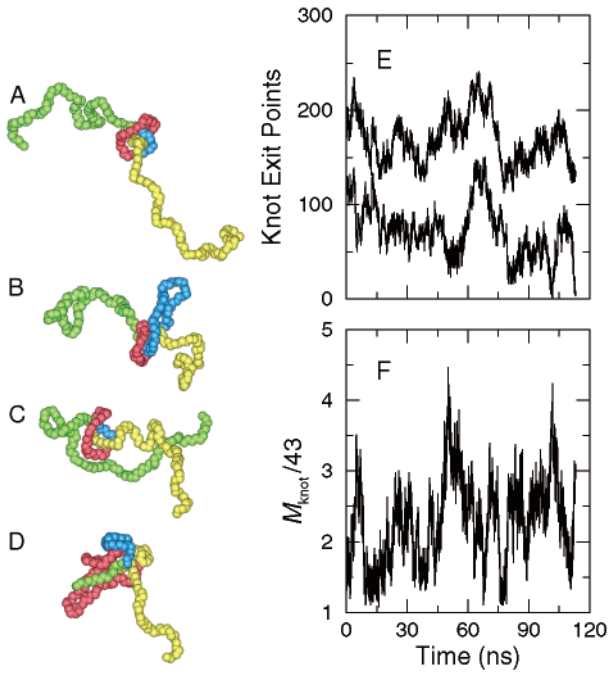

Figure 1. Snapshots of a trefoil-knotted polyethylene chain at different stages of unknotting in a melt of monodisperse chains (C_{209}) at 448 K. The neighboring unknotted chains are not shown. Each sphere of the chain depicts a backbone C atom. (a) At time $t = 0$, one of the chains contains a tight open trefoil knot, highlighted in red and blue, at the middle of the chain. (b) The knot loosens by feeding itself with segments from the arms (yellow and green) to form a hairpin (blue). The number of C atoms in this hairpin is 44. (c) The knot tightens by losing the slack portion (or hairpin) back to the arms. (d) Through cycles of (b) and (c), the knot ultimately slips off one chain end (green). An unknotting trajectory for a longer chain (C_{293}) is plotted for (e) the knot exit points on the chain and (f) the knot size M_{knot} normalized by the tightest knot size, 43. Note that the knot remains finite in size and still tightens down to $M_{knot} = 47$ (at 67 ns) after having expanded up to over 180 or 4 times the original knot size (at 50 ns), which is more than 60% of the overall chain length.

Results and Discussion. Figure 1a−d shows a series of snapshots capturing the essential features of the unknotting process in a polymer melt. Specifically, a trefoil knot that was initially tied securely at the center of the chain loosens by threading segments of the dangling arms into the knot and then tightens by pulling in the slack. With these two as basic moves, the knot migrates along the chain until it slips off one end.

The unraveling process can be quantified by following the locations of two exit points of the knot and the knot size as a function of time. To do so, one needs a definition of the knotted portion of an open knot. Taylor[4] has shown how open knots can be rigorously defined.

† Current address: School of Chemistry and Biochemistry, Georgia Institute of Technology, Atlanta, GA 30332.

10.1021/ma035100e CCC: $27.50
Published on Web 02/07/2004

Here, we use Taylor's chain smoothing algorithm to identify the shortest portion of the chain that retains the knot. The two knot exit points and knot size are defined accordingly, being the indices of the terminal carbon (C) atoms of the knotted portion and the number of C's between the two termini, respectively. Figure 1e,f shows the knot exit points and knot size plotted against time for one of the samples with chain length $M = 293$.

The most prominent geometric feature of the unknotting mechanism is the long hairpin-like structure[21] formed by a growing slack within the knot. This seemingly highly improbable intramolecular arrangement for a strand in the melt—or a strand in a random-coil conformation—allows no neighboring chain segments to intervene between the juxtaposed legs of the hairpin. Evidently, in an extremely slow relaxing network, where no strand passage is allowed across neighboring chains, the only possible way to loosen a slack within the knot will be through forming a hairpin. Opening up the hairpin would require a nearby chain end or tight fold from a neighboring unknotted chain, both of which are highly unlikely. Although the hairpin geometry is directed by intermolecular topological constraints, no hairpin will grow if knot expansion is not driven strongly enough to proceed despite entropic loss associated with the geometry of a hairpin. Multiple hairpins can also grow from a single knot with increasing chain length.

The observation of knot tightening may seem counterintuitive; common experience with macroscopic knots on a rope would not advise us to tighten the knot in order to unravel it. Then, after having expanded to, say, more than 4 times the initial knot size (Figure 1f), why does a knot spontaneously tighten itself down to near its original size, namely the tightest knot size attainable by pulling a free knotted strand on both ends without introducing an excessive strain to the knotted portion? The tightening process can be rationalized in the same context as for hairpin formation: as the slack grows, entropic frustration in its hairpin conformation imposed by intermolecular constraints becomes so overwhelming that the slacked portion is pulled in. The almost full recovery of the tightest knot size is possible because the hairpin remains closed throughout unknotting.

The "local" entanglement effects—in analogy to the entanglement effects in reptation dynamics[5] that are present only in polymers of chain length typically 5 times longer than the entanglement length (approximately C_{100} for PE)—are also evident when the calculated unknotting time τ_u is plotted against chain length M. As shown in Figure 2a, τ_u scales with an exponent of 2.5, i.e., τ_u (ps) $= (0.079 \pm 0.018)(M - \langle M_{knot} \rangle)^{2.5 \pm 0.1}$, where $\langle M_{knot} \rangle$ is the average knot size for each chain length. A smaller scaling exponent of 2 was obtained previously for an isolated granular chain on a vibrating plate.[12] From the tight structure of the hairpin, the local entanglement length may be estimated to be of the order of the monomer size.

The unknotting time, or roughly the time taken for a knot to travel only half the chain length, is great in magnitude when compared to relaxation times of an unknotted, or unperturbed, chain. For instance, τ_u for C_{293} is only an order of magnitude smaller than the longest relaxation time of ~760 ns in the melt.[22] The slow unknotting or enhanced knot security in the melt comes from the controlled unknotting mechanism, rather than from the knot being tangled with other strands. The presence of multiple knots or more complex knots

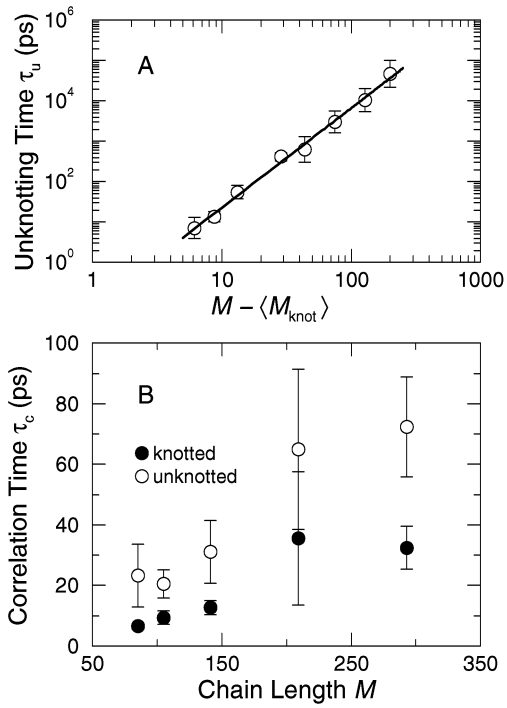

Figure 2. (a) Calculated dependence of the unknotting time τ_u on polymer chain length M. The fitted line follows a power law $\tau_u \sim (M - \langle M_{knot} \rangle)^{2.5}$, where $\langle M_{knot} \rangle$ is the average knot size for each chain length. (b) Effect of unknotting on the orientational relaxation of C−H bond vectors. The correlation time τ_c of the second-order orientation autocorrelation function is obtained by averaging over all C−H bond vectors in the knotted chain or in the unknotted chains. C−H bonds were reconstructed from two backbone C−C bonds flanking the same C atom. The existence of a knot accelerates the local relaxation process, but the resulting memory effect can last as long as the longest relaxation time for an unknotted polymer chain in the melt.

on the chain would likely increase the security of each knot even further.

In contrast to the long lifetime of a tight knot, untying accelerates the local segmental dynamics of the knotted chain. This is also contrary to the common notion of a slowing down in knotted chains,[13] which is also observed in our case when the mean-square displacement is calculated for individual backbone atoms in the knotted chain (data not shown). Figure 2b shows how unknotting affects the orientational relaxation of individual C−H bond vectors, which ^{13}C NMR experiments measure. The faster decay can be understood from our earlier discussion of the slithering motion of segments during expansion and contraction. Taken together, our findings in Figure 2 may provide a scenario for a molecular mechanism underlying the self-contradictory observations often made in NMR experiments,[23] namely that the local dynamics of chain molecules is anomalously fast in some melts with thermal history although the resulting memory effects persist for several days, much longer than the terminal relaxation time of the polymer ($\ll$1 s).

Figure 2b also indicates that the effect of unknotting on local dynamics, averaged over the entire chain the knot is tied into, does not become trivial with increasing chain length. This is not only because the knot, while maintaining its size around a finite value in the course of untying, grows in average size with chain length, that is, $\langle M_{knot} \rangle = (9.5 \pm 0.7)M^{0.4}$, as shown in Figure 3a, but also because the slithering motion associated with the

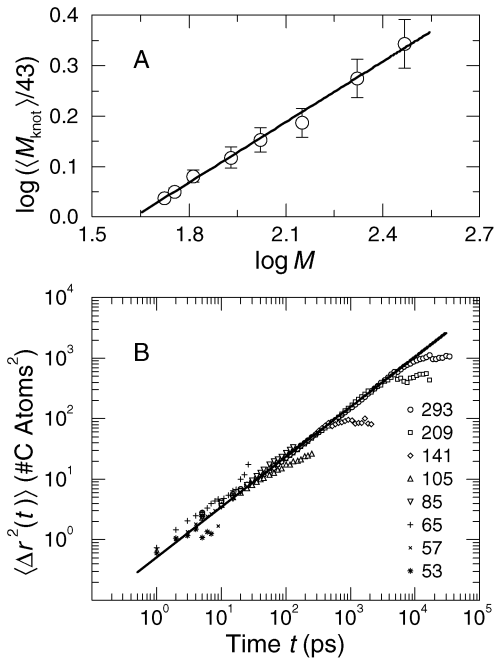

Figure 3. (a) Chain length dependence of the average knot size, $\langle M_{knot}\rangle \sim M^{0.4}$. (b) Plots of the mean-square displacement $\langle \Delta r^2(t)\rangle$ of the knot along the chain for different chain lengths. The center of the knot at time t, or $r(t)$, is defined as an arithmetic average of the two knot exit points. Despite the chain length dependence of the average knot size, the early portions of $\langle \Delta r^2(t)\rangle$ for different knot sizes form a master curve. The black solid line is a fit to the superimposed portions, giving a power law, $\langle \Delta r^2(t)\rangle \sim t^{0.8}$.

expansion/contraction modes does not slow down with increasing knot size, as will be seen in the following discussion. The same $M^{0.4}$ scaling of the knot size was reported in a recent MC simulation study of an isolated knotted chain tethered at both chain ends to two infinite parallel walls.[24] This agreement may be expected because the knot size remains constant in the melt as if two ends of the knotted chain were held apart at a fixed distance.

Figure 3b shows the mean-square displacement $\langle \Delta r^2(t)\rangle$ of the knot along the chain (see the caption of Figure 3 for the definition). The early stage of each curve, which lengthens with chain length, can be described by a single master curve, $\langle \Delta r^2(t)\rangle = 0.52t^{0.8}$. The superposition in this subdiffusive regime indicates the expansion/contraction process of a knot is dictated by the same slithering motion whether the knot is small or large. A crossover to the slow regime for each of the three longest chains, found at about half of the hairpin size, or $(\langle M_{knot}\rangle - 43)/2$, is considered a manifestation of the finite knot size. The slow second regime stretches to the unknotting point in the mean-square displacement plot (only half of the entire trajectory for each chain length is shown here) and corresponds to the migration of the knot along the chain. The absence of a crossover or second regime for shorter chains is attributed to the progressively poorer sampling with decreasing chain length.

The knot size-independent expansion/contraction mechanism, along with the chain length-dependent knot size, results in an unusual chain length dependence of the slithering dynamics. At an arbitrary time between two neighboring crossover points in Figure 3b, the one-dimensional mean-square displacement is larger for the longer chain than for the shorter. In other words, the longer the chain, the faster the dynamics!

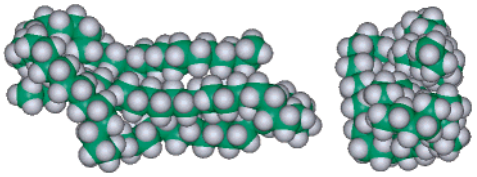

Figure 4. A single chain "lamella" formed by a knotted chain. The snapshot was taken soon after a tight trefoil knot on the C_{85} chain became untied. White spheres represent reconstructed hydrogen atoms. A side view is also shown.

The two scaling laws of Figures 2a and 3b may be drawn from each other, considering that in order for a knot to untie it should travel a distance proportional to $M - \langle M_{knot}\rangle$ and that $r^{2.5} \sim t$ as drawn from the fast regime of the mean-square displacement plot. This suggests that the stronger chain length dependence of τ_u than in the isolated chain may be due to the subdiffusive one-dimensional slithering motion shared by chains with different lengths rather than the increasing knot size with chain length.

A tight knot's ability to fold a stem by forming a hairpin could perhaps play a role in polymer crystallization from the melt. Tight knots, when present in an undercooled melt, could become potential nuclei in the primary nucleation step, which come into action as soon as unknotting begins. The "knot-triggered" nucleation may be regarded as a type of self-nucleation—or nucleation by its own crystals that were grown previously but have survived the dissolution or melting step—and is not unrealistic, considering the critical dimensions of a nucleus for the more difficult homogeneous nucleation, which can be as small as five stems with 40 C's each.[25] The possible role of knots in nucleation is well represented in a snapshot taken right after a typical knot becomes undone (Figure 4). Here, the unknotted chain has been folded into a single chain lamella. The formation of this folded lamella is aided in part by the inherent compactness of the tight knot. The long unknotting time stresses the significance of knots' role in nucleation because the long unknotting time also means a long lifetime for the nuclei.

Hairpin formation and enhanced slithering motion may also be relevant for the supercoiling of DNA[1,26] if our open knot can be viewed to represent a portion of a circular knot to which its knotted region is localized at a particular instant. In the intracellular state, swinging a strand through space in order to bring together two sites from separate locations on a duplex DNA is prohibited unlike in solution. Therefore, hairpin formation as a result of knots interacting topologically with other cellular proteins may be an effective means to promote supercoiling—or winding two strands of duplex DNA around each other—in addition to the instability due to local twisting of duplex DNA,[1,26] preceding biological actions of topoisomerases.[6] In the same context, juxtaposition dynamics of distant sites on supercoiled DNA, which in solution depends on very slow internal slithering of opposite segments along the supercoil axis,[27] may be facilitated.

Conclusions. We used molecular dynamics simulations to explore the dynamical evolution of a trefoil knot tied on a polyethylene chain embedded in a melt of similar but unknotted chains. A tight open trefoil knot unravels via a sequence of expansions and contractions plus migration while maintaining a definite size $\langle M_{knot}\rangle$ that grows with chain length M as $M^{0.4}$. The unknotting time scales as $(M - \langle M_{knot}\rangle)^{2.5}$. The associated slithering

motion is much faster than for an unknotted chain and, together with the hairpin geometry of knot expansion, can provide an efficient means to juxtapose distant sites on the same strand in a dense macromolecular environment.

Acknowledgment. We thank W. L. Mattice, G. J. Martyna, and G. Xu for guidance on the computational algorithms and R. D. Kamien for suggestions. This work was supported by the U.S. National Science Foundation.

References and Notes

(1) Schlick, T.; Olson, W. K. *Science* **1992**, *257*, 1110−1115.
(2) Katritch, V.; Bednar, J.; Michoud, D.; Scharein, R. G.; Dubochet, J.; Stasiak, A. *Nature (London)* **1996**, *384*, 142−145.
(3) Podtelezhnikov, A. A.; Cozzarelli, N. R.; Vologodskii, A. V. *Proc. Natl. Acad. Sci. U.S.A.* **1999**, *96*, 12974−12979.
(4) Taylor, W. R. *Nature (London)* **2000**, *406*, 916−919.
(5) Doi, M.; Edwards, S. F. *The Theory of Polymer Dynamics*; Oxford University Press: New York, 1986.
(6) Champoux, J. J. *Annu. Rev. Biochem.* **2001**, *70*, 369−413.
(7) Janse van Rensburg, E. J.; Sumners, D. A. W.; Wasserman, E.; Whittington, S. G. *J. Phys. A: Math. Gen.* **1992**, *25*, 6557−6566.
(8) de Gennes, P.-G. *Macromolecules* **1984**, *17*, 703−704.
(9) Grosberg, A. Y.; Feigel, A.; Rabin, Y. *Phys. Rev. E* **1996**, *54*, 6618−6622.
(10) Katritch, V.; Olson, W. K.; Vologodskii, A.; Dubochet, J.; Stasiak, A. *Phys. Rev. E* **2000**, *61*, 5545−5549.
(11) Metzler, R.; Hanke, A.; Dommersnes, P. G.; Kantor, Y.; Kardar, M. *Phys. Rev. Lett.* **2002**, *88*, 188101.
(12) Ben-Naim, E.; Daya, Z. A.; Vorobieff, P.; Ecke, R. E. *Phys. Rev. Lett.* **2001**, *86*, 1414−1417.
(13) Lai, P.-Y.; Sheng, Y.-J.; Tsao, H.-K. *Phys. Rev. Lett.* **2001**, *87*, 175503.
(14) Ashley, C. W. *The Ashley Book of Knots*; Doubleday: New York, 1993; pp 16−17.
(15) Pieranski, P.; Kasas, S.; Dietler, G.; Dubochet, J.; Stasiak, A. *New J. Phys.* **2001**, *3*, 10.1−10.13.
(16) Saitta, A. M.; Soper, P. D.; Wasserman, E.; Klein, M. L. *Nature (London)* **1999**, *399*, 46−48.
(17) Arai, Y.; Yasuda, R.; Akashi, K.; Harada, Y.; Miyata, H.; Kinosita, K., Jr.; Itoh, H. *Nature (London)* **1999**, *399*, 446−448.
(18) Martin, M. G.; Siepmann, J. I. *J. Phys. Chem. B* **1998**, *102*, 2569−2577.
(19) Doruker, P.; Mattice, W. L. *Macromol. Theory Simul.* **1999**, *8*, 463−478.
(20) Mattice, W. L.; Suter, U. W. *Conformational Theory of Large Molecules: The Rotational Isomeric State Model in Macromolecular Systems*; Wiley-Interscience: New York, 1994.
(21) Our hairpin is irrelevant to the "arch in a caterpillar" model often used to describe reptation,[5] not only because the latter is on vastly different spatial and time scales but also because the open arch embraces neighboring segments.
(22) Pearson, D. S.; Ver Strate, G.; von Meerwall, E.; Schilling, F. C. *Macromolecules* **1987**, *20*, 1133−1141.
(23) Folland, R.; Charlesby, A. *Eur. Polym. J.* **1979**, *15*, 953−955.
(24) Farago, O.; Kantor, Y.; Kardar, M. *Europhys. Lett.* **2002**, *60*, 53−59.
(25) Welch, P.; Muthukumar, M. *Phys. Rev. Lett.* **2001**, *87*, 218302.
(26) Vologodskii, A. V.; Cozzarelli, N. R. *Annu. Rev. Biophys. Biomol. Struct.* **1994**, *23*, 609−643.
(27) Huang, J.; Schlick, T.; Vologodskii, A. *Proc. Natl. Acad. Sci. U.S.A.* **2001**, *98*, 968−973.

MA035100E